The Effect Of Aeroelasticity Upon Energy Retrieval Of A Sailplane Penetrating A Gust

By H. Ulv Mai

ABSTRACT

The paper, prepared for and presented at the XIX OSTIV Congress, August 2-10, 1985, in Rieti, Italy, discusses the altitude and energy altitude gains of a sailplane penetrating a gust, taking into account the rigid-body motions, and wing bending and twisting. The aerodynamic calculations were performed using quasi-steady strip theory. Gust penetration characteristics of the 15 m span PIK-20 and the 20 m span ALCOR sailplanes have been simulated by means of computer programs and effects of various parameters on the altitude and energy altitude gains are discussed. The simulations show that aeroelasticity has an appreciable effect on the gust penetration behavior of sailplanes, and that the main contributing factors are wing bending in connection with rigid-body pitching.

SYMBOLS

a	lift-curve slope		t	time
A	aspect ratio		T	thrust
c	local chord		$\hat{u}$	dimensionless velocity
$\bar{c}$	mean aerodynamic chord		V	flight speed
C_L	lift coefficient		V_H	tail volume ratio (see Eq. 13)
$C_{..}$	stability derivative		w	vertical speed
D	drag		w_g	gust speed
$\bar{D}$	derivative operator		w_{gn}	nominal gust speed
e	Oswald factor		W	airplane weight $= mg$
f	spring constant		x	horizontal distance
g	acceleration due to gravity		z	vertical displacement
h	c.g. location in parts of $\bar{c}$		z_e	energy altitude change
h_n	stick-fixed neutral point, parts of $\bar{c}$		α	angle of attack
i_B	dimensionless moment of inertia about spanwise axis		γ	flight path slope
j_y	radius of gyration about spanwise axis		δ_c	(see Fig. 9)
k_{ij}	stiffness matrix element		δ_e	(see Fig. 9)
l_t	tail arm length		$\Delta(\ )$	difference from the steady value
L	lift		θ	angle of pitch
L_{gn}	nominal gust length		μ	mass ratio (see Eq. 6)
m	airplane mass		ρ	density of air
n	number of wing elements		$(\ )_i$	element i value
q	kinetic pressure		$(\ )_t$	tail value
S	wing area		$(\ )_o$	steady-state value

INTRODUCTION

The origin of the present paper lies within an observation made by Robert Lamson at the end of the 1970's. When flying his ALCOR sailplane in formation with a PIK-20 through gusty air he found himself gust by gust higher than the PIK-20. This happened without any conscious controlling with the stick. When penetrating the gust he also felt a gentle forward push. These observations led to the assumption that a sailplane may, by aeroelastic or other means, be able to absorb energy from gusts without pilot interference, and that this ability might be different for different airplanes and configurations.

This consequently led to a number of further questions, such as (a) which are the determining factors in a sailplane's ability to absorb energy from gusts and (b) how could a sailplane be tailored so as to maximize this ability.

The present paper is an attempt to find answers to these questions, and to describe the phenomenon and the governing factors therein. To this end the gust response of two airplanes was analyzed. The first of these, the PIK-20, is a 15 m class sailplane; the other, the ALCOR, is a 20 m span, 28:1 aspect ratio sailplane especially designed for high altitude flight. The analysis was performed under some simplifying assumptions described in detail below.

The point of view of the paper is, in a way, converse to that of the theory of optimal dolphin-type flight. In the latter the task is to find flight techniques so as to maximize the average speed, without total energy loss, when flying through gusty air. On the other hand, in the present investigation the objective is to find ways of maximizing total energy gain of a glider penetrating a gust, without any pilot interference.

THE THRUST EFFECT

The effect of an upward gust upon a glider is twofold. First, the lift is increased due to increase of the angle of attack. Second, the lift vector is tilted forward. This is based on the fact that the lift is, by definition, always perpendicular to the instantaneous direction of the onset flow. An upward gust causes a change in the direction of the onset flow without an immediate change in the direction of motion of the vehicle; thus the lift vector has a component in the direction of motion, which is felt as an

$\vec{\Delta T}$ = the apparent thrust

$\vec{L}_o + \vec{\Delta L}$ = the lift vector under the influence of a gust

$\vec{L}_o$ = the steady-state lift vector

$\vec{V}_o$ = the steady state flight speed

$\vec{w}_g$ = the gust speed

$-\vec{V}$ = the onset flow speed under the influence of a gust

FIGURE 1: Effect of an upward gust on the lift vector
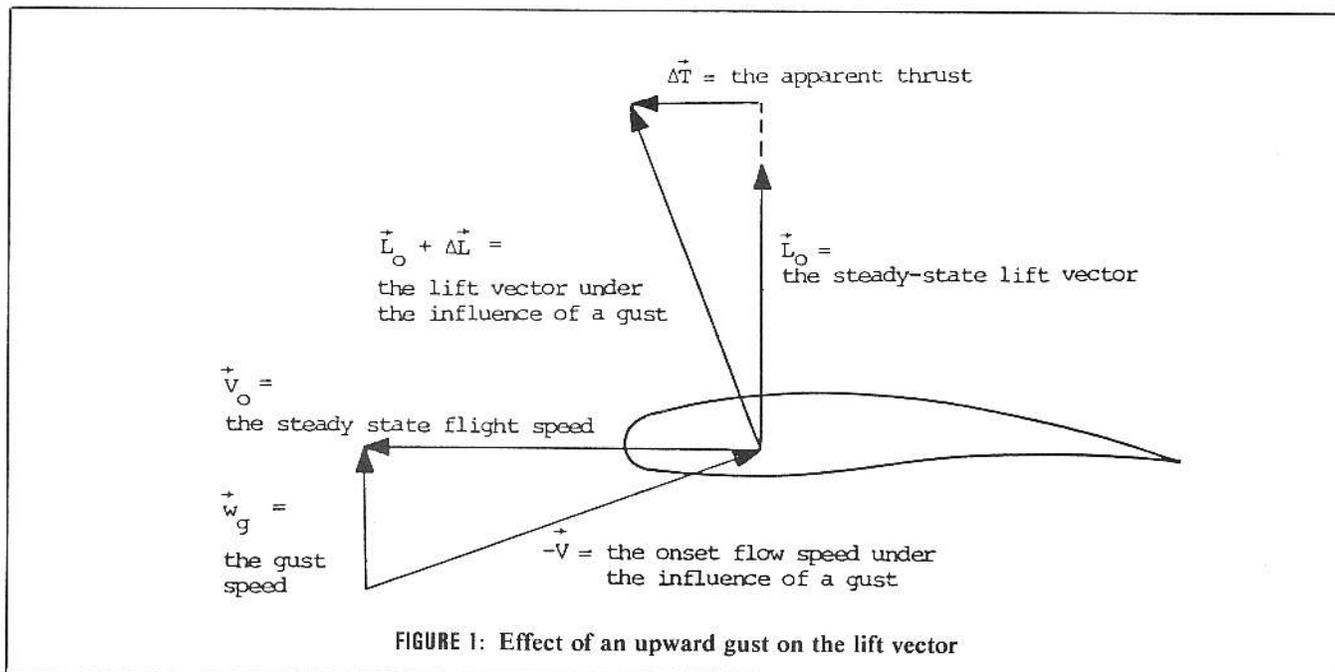
apparent thrust (see **Figure 1**). The phenomenon is described by the force equilibrium in the instantaneous flight direction

$$(1) \quad T - D + L(w_g/V) - mg \sin \gamma - m\dot{V} = 0$$

where T is the thrust (zero for a sailplane), D is the drag, L the lift, w_g the gust velocity normal to the flight path, V the flight speed, m airplane mass, g the acceleration due to gravity, γ the inclination of the flight path (positive for rising flight paths), and $\dot{V}$ the acceleration. As is seen, an upward gust causes a force unbalance felt as apparent thrust.

The lift increase also causes the induced drag to increase by the amount

$$(2) \quad \Delta D = \frac{(\Delta L + L_o)^2 - L_o^2}{qS\pi Ae} = \frac{2\Delta LC_{Lo}}{\pi Ae}$$

where ΔL is the increase in lift, L_o the original equilibrium lift equalling airplane weight W, q the kinetic pressure, S the wing area, A the aspect ratio, e the Oswald factor and C_{Lo} the equilibrium lift coefficient. The acceleration caused by the combined thrust and drag increase effects is then

$$(3) \quad \dot{V} = \frac{gw_g}{V} - \frac{2gaw_g}{V\pi Ae} = g\left[1 - \frac{2a}{\pi Ae}\right]\frac{w_g}{V}$$

where a is the lift-curve slope.

As soon as the lift builds up the airplane begins to move upward so as to cancel the gust effect. The phenomenon is thus highly transient.

In a down gust the lift vector is tilted backward which causes a "negative thrust". However, the lift vector is also decreased in magnitude; this means that the "negative thrust" experienced in a down gust is smaller than the corresponding "positive thrust" caused by the upward gust. Thus an airplane flying through gusty air experiences a small positive net thrust. This phenomenon, sometimes called the Katzmayer effect, is usually considered to be negligible from a performance point of view. However, the calculations discussed in the next chapters show that, to

some extent, wing flexibility may strengthen this effect.

To gain more insight to the problem, let us first see how the gust affects a rigid sailplane penetrating an upward gust.

A RIGID SAILPLANE PENETRATING A SINUSOIDAL GUST

According to Etkin[2] the basic equations describing the symmetric motions of an airplane disturbed from equilibrium flight can be written in the form

$$(4a) \quad (2\mu\bar{D} - 2 C_{Lo}\tan\gamma - C_{xu})\hat{u} - C_{x\alpha}\alpha + C_{Lo}\theta = 0$$

$$(4b) \quad (2 C_{Lo} - C_{zu})\hat{u} + (2\mu\bar{D} - C_{z\dot{\alpha}}\bar{D} - C_{z\alpha})\alpha$$
$$- \left[(2\mu + C_{zq})\bar{D} - C_{Lo}\tan\gamma\right]\theta = 0$$

$$(4c) \quad -C_{mu}\hat{u} - (C_{m\dot{\alpha}}\bar{D} + C_{m\alpha})\alpha + (i_B\bar{D}^2 - C_{mq}\bar{D})\theta = 0$$

where $\hat{u} = \Delta V/V_o$ is the dimensionless velocity disturbance, α is the angle of attack disturbance, and θ the pitch angle disturbance, all assumed to be small; γ is the initial flight path slope. Further, i_B is the dimensionless moment of inertia,

$$(5) \quad \bar{D} = \frac{\bar{c}}{2V}\frac{d}{dt}$$

The dimensionless derivative operator,

$$(6) \quad \mu = \frac{2m}{\rho S\bar{c}}$$

is aircraft mass ratio, and C subnotes are stability derivatives. In Eq. (6) m is airplane mass, ρ is the density of the air, S the wing area and c the mean aerodynamic chord. Eq. (4a) represents the force equilibrium tangential to the flight path, Eq. (4b) the force equilibrium normal to the flight path and Eq. (4c) the moment equilibrium about the spanwise axis (pitch axis).

If the airplane is crossing a gust field with gust velocity

w_g then the instantaneous angle of attack consists of three parts as follows:

(7)
$$\alpha = \frac{w_g}{V} - \frac{w}{V} + \theta \approx \frac{w_g}{V_o} - \frac{w}{V_o} + \theta$$

where w is the upward velocity. It will be shown later on that the relative changes in flight velocity are small; thus the approximation shown in the latter part of Eq. (7) is justified. For the same reason the kinetic pressure q can be replaced by the equilibrium kinetic pressure q_o.

For a high performance sailplane the glide is very shallow; then the terms containing $\tan \gamma$ can be neglected in Eqs. (4). Likewise, the stability derivatives C_{xu}, C_{zu} and C_{mu} are very small and can be neglected. For sailplanes with a large aspect ratio and consequently a small downwash derivative the terms $C_{z\dot\alpha}\overline{D}$ and $C_{m\dot\alpha}\overline{D}$ can be neglected in comparison with $C_{z\alpha}$ and $C_{m\alpha}$, respectively. For the remainder the following approximations apply (see Etkin[2]):

(8)
$$C_{x\alpha} = C_{Lo} - \frac{2C_{Lo}}{\pi Ae}\, a$$

(9)
$$C_{z\alpha} = -a$$

(10)
$$C_{zq} = -2\, a_t V_H$$

(11)
$$C_{m\alpha} = -a(h_n - h)$$

(12)
$$C_{mq} = -2\, a_t V_H (l_t/\overline{c})$$

where a_t is the tail lift-curve slope,

(13)
$$V_H = \frac{S_t l_t}{S\overline{c}}$$

the tail volume ratio and $(h_n - h)$ the static stability margin in parts of $\overline{c}$: S_t is the tail area and l_t the tail moment arm length from the c.g.

Substituting these expressions in Eqs. (4) and taking the aforementioned simplifications into account we get the following equations of motion:

(14a)
$$\Delta\dot{V} = \left[g - \frac{2ga}{\pi Ae}\right]\left[\frac{w_g}{V_o} - \frac{w}{V_o}\right] - \frac{2ga}{\pi Ae}\theta$$

(14b)
$$\dot{w} = \frac{2g}{V_o}\Delta V - \frac{ga}{V_o C_{Lo}}w + \frac{ga}{C_{Lo}}\theta + \frac{ga}{V_o C_{Lo}}w_g$$

(14c)
$$\ddot{\theta} = -\frac{ga}{V_o C_{Lo}\overline{c}(j_y/\overline{c})^2}\left[\frac{a_t}{a}V_H l_t\dot{\theta} + (h_n - h)w_g\right.$$
$$\left. - (h_n - h)w + (h_n - h)\theta V_o\right]$$

These equations can be integrated, by numerical or other means, to obtain the motion of the airplane as a function of time in response to a given gust field. $V = V_o + \Delta V$ and w can further be integrated to yield the altitude increase z and distance x flown:

(15a)
$$\frac{dz}{dt} = w$$

(15b)
$$\frac{dx}{dt} = V + \Delta V$$

The total energy altitude increase z_e can then be obtained from

(16)
$$z_e = \frac{1}{mg}\left(\frac{1}{2}mV^2 + mgz - \frac{1}{2}mV_o^2\right) = \frac{1}{2g}(V^2 - V_o^2) + z$$

For the present report a computer program GUST0 doing these calculations was written for the Hewlett-Packard 9816 computer[1]. This program uses a fourth order Runge-Kutta scheme to find the response of a rigid sailplane to a given gust.

In the present investigation a sinusoidally distributed up gust was used as shown in **Figure 2**. The mathematical expression of the gust is

(17)
$$w_g = .5\, w_{gn}\left[1 + \sin(2\pi x/L_{gn} - \pi/2)\right]; \quad 0 < x < L_{gn}$$

where w_{gn} is the nominal gust speed and L_{gn} the gust length.

A number of numerical experiments were undertaken with program GUST0 to find the effect of various factors to the gust response. It seems that the most important single parameters, for given flight speed, are static stability margin, and radius of gyration of the sailplane.

---

[1]The computer programs, including GUST0, referred to in this paper are available on request from the author.
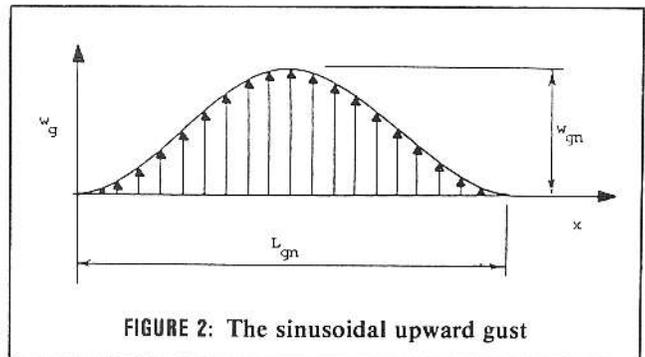
FIGURE 2: The sinusoidal upward gust

The effect of the wing loading seems to be quite small. Some calculations were made for the "rigid" PIK-20 (**Figure 3**) in a gust of form (17) of nominal strength 2 m/s and length 50 m, with a nominal flight speed of 40 m/s. Pertinent data of the sailplane are shown in **Table I** below.

TABLE I: Physical characteristics of the PIK-20 glider

Wing area	S	10.00 m^2
Wing span	b	15.00 m
Aspect ratio	A	22.50
Taper ratio		0.40
Mean aerodynamic chord	$\overline{c}$	0.7025 m
Oswald constant	e	0.80
Overall lift-curve slope	a	5.80
Tail lift-curve slope	a_t	3.47
Tail volume ratio	V_H	0.51
Tail length ratio	$l_t/\overline{c}$	5.224
Total mass	m	350 kg
Dimensionless radius of gyration	$i_y/\overline{c}$	100 %
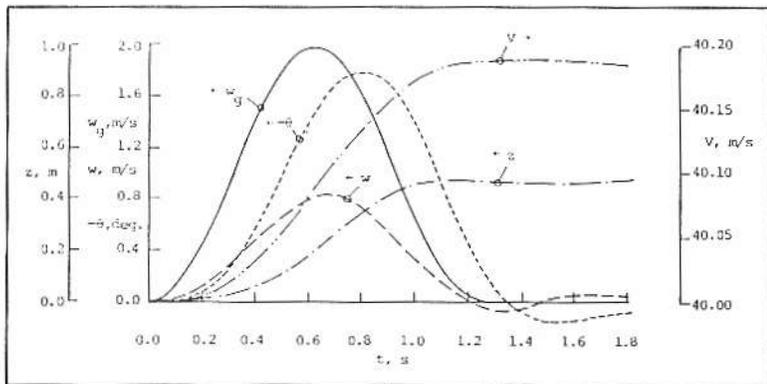
FIGURE 3:

FIGURE 3: Results of a sample calculation with
GUST0 for PIK-20. m = 350 kg,
c.g. margin = 20% of $\bar{c}$, w_{gn} = 2 m/s,
L_{gn} = 50 m, V_o = 40 m/s;
calculated z_e = 1.251 m
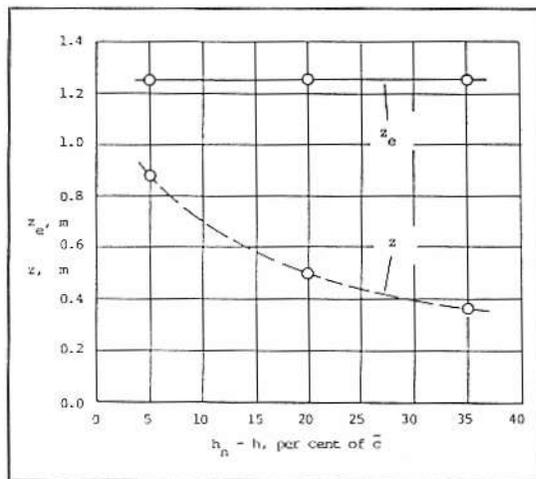
FIGURE 4: Effect of static stability margin on
the altitude, velocity and total energy gain
of the PIK-20. w_{gn} = 2 m/s,
L_{gn} = 50 m, V_o = 40 m/s

Figure 4 clearly shows that the altitude gain increases
with diminishing static stability margin (i.e. with center of
gravity moving backward). This depends on the dimin-
ishing weathercock effect. On the other hand, the thrust
effect simultaneously diminishes accordingly. Surprisingly
enough, for the sailplane investigated the c.g. location does
not seem to have any visible effect on the energy altitude
increase. It is not known whether or not this is a pure
coincidence or an indication of a general property.

The calculations also confirm the assumption of a small
velocity increase V. However, there can be quite large
differences in the altitude increase between various air-
planes, depending on the configuration and loading condi-
tion. In the case depicted in Figure 3 the apparent thrust
follows roughly the upward gust speed, the maximum value
being 99 N at 0.63 s from gust onset.
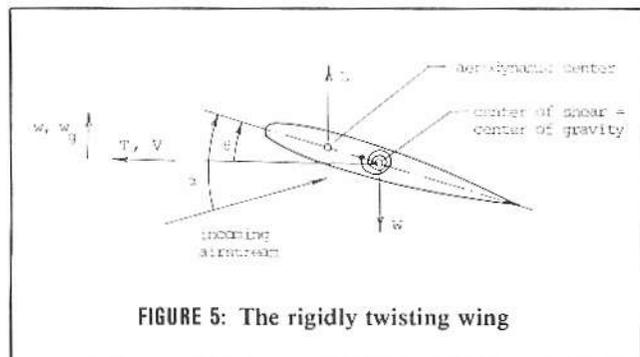
FIGURE 5: The rigidly twisting wing

FIGURE 4:

THE RIGIDLY TWISTING WING

To move to aeroelastic effects let us first consider the
behavior of a glider having a rigid wing which is able to
twist with respect to the fuselage (see Figure 5). The wing is
assumed to be attached to the fuselage via a torsion spring
in such a manner that a lift L causes the wing to twist by an
amount $\theta = fL$.

In this case the instantaneous angle of attack is

(18)
$$\alpha = \alpha_o + \frac{w_g}{V} - \frac{w}{V} + \theta = \alpha_o + \frac{w_g}{V_o} - \frac{w}{V_o} + fL$$

where α_o is the steady, unelastic equilibrium angle of
attack prior to entering the gust.

Thus the instantaneous lift is

(19)
$$L = \frac{1}{2}\rho V^2 Sa\alpha = qSa\left(\alpha_o + \frac{w_g}{V_o} - \frac{w}{V_o} + fL\right)$$
$$= \frac{qSa(\alpha_o + w_g/V - w/V)}{1 - qSaf} \approx \frac{q_o Sa(\alpha_o + w_g/V_o - w/V_o)}{1 - q_o Saf}$$

The latter form of Eq. 19 follows from the fact that velocity
increases are very small compared to V_o.

It is worthy of noticing that for the condition

(20) $qSaf = 1$

the lift becomes singular, indicating aeroelastic divergence.

The steady angle of attack α_o can be solved from the
condition that prior to entering the gust the lift must equal
the weight W. Thus

(21)
$$W = \frac{q_o Sa\,\alpha_o}{1 - q_o Saf}$$

Solving Eq. (21) for α_o and substituting the result in Eq.
(19) gives the following equation for L:

(22)
$$L = \frac{q_o Sa(w_g - w)}{V_o(1 - q_o Saf)} + W$$

Note that the lift increase over W can be very large if the
speed is close to the divergence speed.

In the present case the thrust due to forward tilting of the lift vector is

$$(23) \quad \Delta T = L \, \frac{w_g - w}{V_o}$$

and the increase in the induced drag

$$(24) \quad \Delta D = \frac{(L^2 - w^2)}{q_o S \pi A e}$$

Thus the net thrust is

$$(25) \quad T = \Delta T - \Delta D = L \, \frac{w_g - w}{V_o} - \frac{(L^2 - w^2)}{q_o S \pi A e}$$

It is now possible to formulate the equations of motion in the vertical direction as follows:

$$(26a) \quad \frac{dw}{dt} = \frac{L - w}{m}$$

$$(26b) \quad \frac{dV}{dt} = \frac{T}{m}$$

where L and T are given by Eqs. (22) and (25), respectively. Eqs. (26) can be integrated numerically to give w and V, as well as z and x as functions of time.

These calculations were again performed by a computer program named GUST1 with the HP 9816 computer. Some of the results are shown in Figures 6a and 6b. They show w, w_g, V and z as functions of time for a sailplane penetrating a sinusoidal gust of magnitude 2 m/s and length 50 m, with an initial speed 40 m/s. Other data were as given in Table I except that the lift-curve slope was assumed to be 6.283.
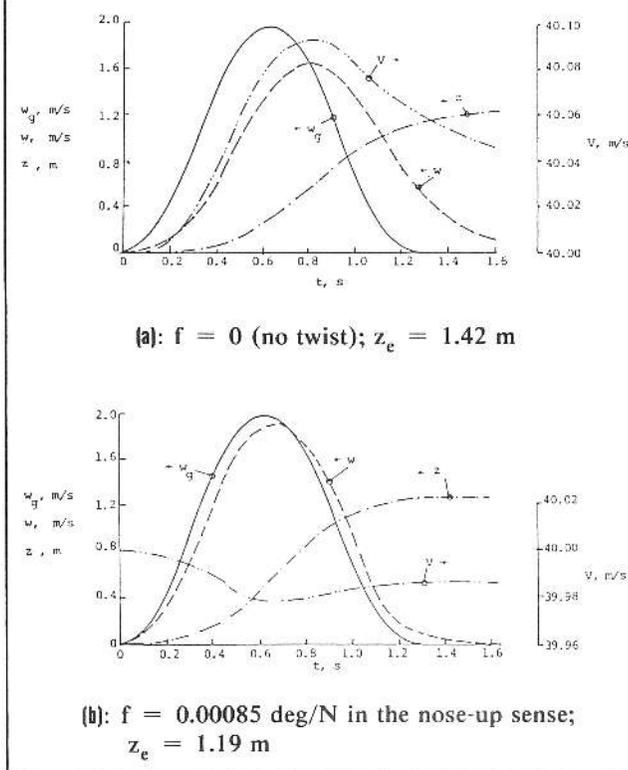
Figure 6a shows the case when $f = 0$, i.e. the wing does not twist at all due to lift, and Figure 6b the case $f = 0.00085$ deg/N (that is, a common nose-up twist due to lift increase). It is seen that the velocity change is small in both cases. However, even if numerically small, the velocity change accounts for almost all of the difference in total energy gain, since the geometric altitude increase is practically the same in both cases.

The inferior energy gain of the case depicted in Figure 6b appears to be caused by the following phenomena: As the airplane enters the gust the lift increases very rapidly due to aeroelastic twisting of the wing. This lift buildup causes the plane to hump upward very rapidly, thus virtually eliminating the angle of attack increase due to the gust and the accompanying forward tilt of the lift vector. Simultaneously the high lift causes a large increase in the induced drag. These effects together cause the net thrust to vanish altogether (and even to change sign), and a drop in velocity follows.

Figure 7 shows the energy altitude increase as a function of the spring constant f for the same glider. It is seen that for typical values of f the wing twist due to lift has a small
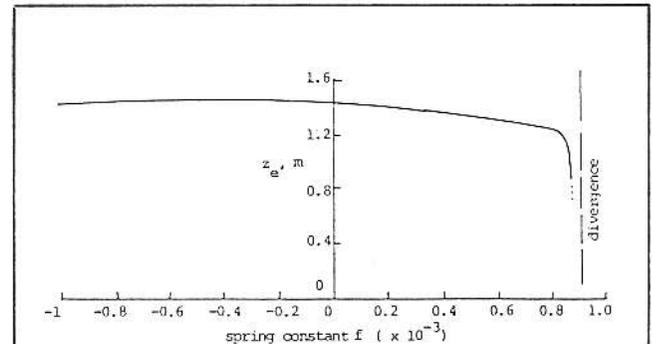
FIGURE 7: Energy altitude increase as a function of the spring constant f

but clear effect on the altitude gain. The latter has a maximum at a moderate negative value of f. Near the divergence value (corresponding to the case where the initial velocity V_o is the divergence speed for the given spring constant f) the energy gain begins to drop off very rapidly.

The lesson learned from this is that if the wing twist due to lift can be controlled by structural means, then positive values of f should be avoided, optimum being a small negative value. Physically this means that an increase in lift should cause a nose-down twist of the wing. This again implies that the center of shear should be in front of the aerodynamic center axis of the profile—a condition which is quite difficult to attain by conventional materials and construction principles. However, with aeroelastic tailoring this condition can be fulfilled.

FIGURE 6: Effect of f on the hypothetical rigidly-twisting-wing sailplane penetrating a gust

(a): f = 0 (no twist); $z_e = 1.42$ m

(b): f = 0.00085 deg/N in the nose-up sense; $z_e = 1.19$ m
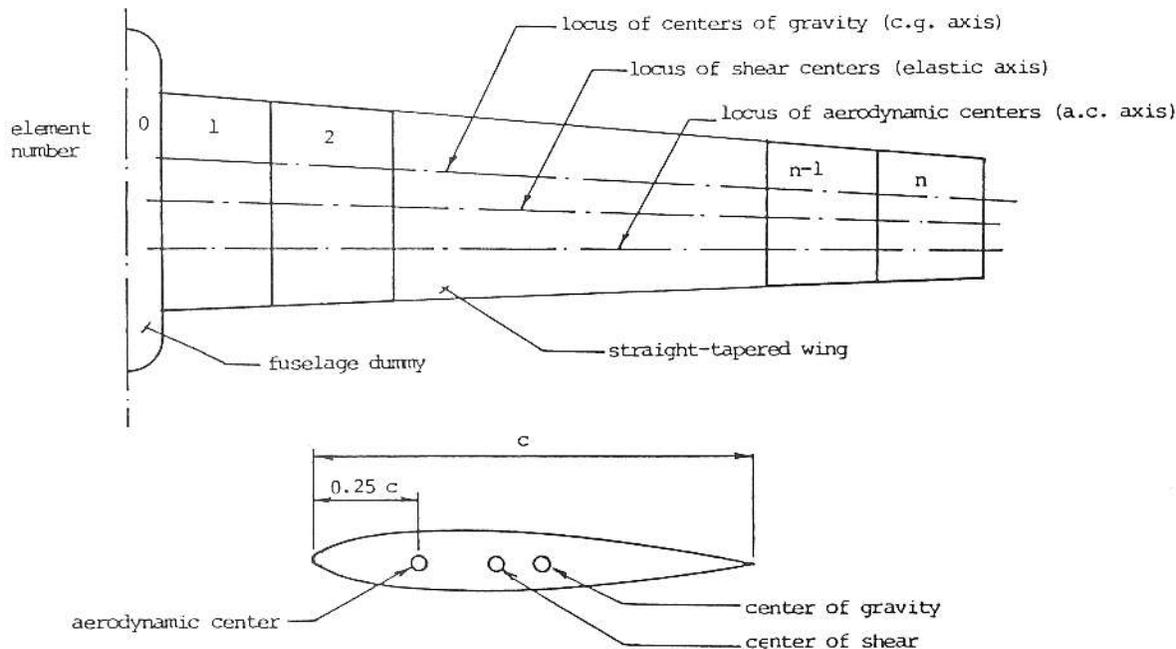
FIGURE 8: The model used in the analysis of the elastic sailplane

THE SAILPLANE WITH AN ELASTIC WING

The gust response of the sailplane with an elastic wing was computed by means of an element method developed especially for the present paper. To this end the wing was divided into a number of spanwise elements numbered consecutively from 1 to n from root to tip (see **Figure 8**). In the calculations discussed later, nine wing elements were used. The fuselage was represented by an element having the mass, the moment of inertia and roughly the aerodynamic properties of the fuselage-tail combination (see **Figure 8**). This element was given the number 0.

For simplicity the wing planform was approximated by a straight-tapered trapezoid. Each wing element was characterized by the center of shear, the center of gravity and the aerodynamic center, the latter being located at the 25% point of the local chord. The loci of centers of shear (the elastic axis), the centers of gravity (the center of gravity axis) and the aerodynamic centers (the aerodynamic axis) were assumed to be straight lines. Each wing element was assumed to have a given mass concentrated at the local c.g., and a given radius of gyration, the latter being a given percentage of the local chord.

The position of each element (including wing elements and the "fuselage") was determined by two parameters, viz., (a) the vertical displacement z_i of the element c.g. from the original, equilibrium position and (b) the angular displacement θ_i with respect to the local c.g. (see **Figure 9**).

Aerodynamic forces and inertia forces were assumed to be acting on the aerodynamic center and the center of gravity, respectively. Twisting was assumed to occur about the elastic axis (that is, a pure torque was assumed not to cause any vertical displacement of the elastic axis). The downwash control point was assumed to be the 75% point of the local chord.

Under these assumptions the equations of motion of the element system can be written as follows:

(27a)
$$\ddot{z}_i = \left\{ -\sum_{j=0}^{n} k_{ij} z_j - \sum_{j=n+1}^{2n+1} k_{ij} \theta_{j-n-1} + q_o S_i a \left[\theta_i - \frac{\dot{z}_i}{v_o} + \delta_{ci} \frac{\dot{\theta}_i}{v_o} \right] \right\} \frac{1}{m_i} \quad (i = 1 \ldots n)$$

(27b)
$$\ddot{z}_0 = \left\{ -\sum_{j=0}^{n} k_{0j} z_j - \sum_{j=n+1}^{2n+1} k_{0j} \theta_{j-n-1} \right\} \frac{1}{m_0}$$

(27c)
$$\ddot{\theta}_i = \left\{ -\sum_{j=0}^{n} k_{i+n+1,j} z_j - \sum_{j=n+1}^{2n+1} k_{i+n+1,j} \theta_{j-n-1} - d k_{i+n+1,i+n+1} + q_o S_i a \delta_{ei} \left[\theta_i - \frac{\dot{z}_i}{v_o} + \delta_{ci} \frac{\dot{\theta}_i}{v_o} \right] \right\} \frac{1}{j_{yi}^2 m_i} \quad (i = 1 \ldots n)$$

(27d)

$$\ddot{\theta}_0 = \left\{ -\sum_{j=0}^{n} k_{n+1,j} z_j - \sum_{j=n+1}^{2n+1} k_{n+1,j} \theta_{j-n-1} \right\} \frac{1}{j_y^2 \, m}$$

$$- \frac{g a_t V_H l_t}{V_o C_{Lo} \bar{c} (j_y / \bar{c})^2} \dot{\theta}_0 - \frac{(h_n - h) \bar{c} (L - W)}{j_y^2 \, m}$$

where m_i is the mass of the element, i, k_{ij} are elements of the free-body stiffness matrix, z_i is the vertical displacement of element i, θ_i the angular displacement of element i, and j_{yi} the radius of gyration of element i. The dots above a symbol denote differentiation with respect to time. Further, δ_{ci} and δ_{ei} are the distances of the local c.g. axis behind the 75% point of the chord and distance of the local elastic axis behind the local aerodynamic center, respectively (see **Figure 9**). L is the total lift which is computed according to Eq. (31).

Eqs. (27) give the vertical force and pitching moment equilibrium for elements 0 ... n. In addition to these the horizontal force equilibrium is needed. This is simply,

(27e) $\quad m \, \ddot{x} = T$

where m is the total mass of the airplane, $\ddot{x}$ the horizontal acceleration and T the net thrust. The latter can, in turn, be calculated from

(28)

$$T = 2 \sum_{i=1}^{n} L_i \Delta\alpha_i - \frac{2W (L - W)}{q_o S \pi A e}$$

where

(29) $\quad L_i = q_o S_i a \, (\Delta\alpha_i + \alpha_o + \theta_i)$

is the lift acting on element i,

(30)

$$\Delta\alpha_i = \frac{w_g - \dot{z}_i + \dot{\theta}_i \delta_{ci}}{V_o}$$

is the angle of attack disturbance due to the gust and due to wing motions,

(31)

$$L = 2 \sum_{i=1}^{n} L_i$$

is the total lift and

(32)

$$\alpha_o = \frac{W}{q_o S a}$$

is the equilibrium angle of attack.

Eqs. (27) deserve a couple of comments and explanations. The first two terms in the right-hand sides of Eqs. (27a) and (27b) represent the elastic restraint force acting on element i. The third term represents the lift due to element motions and displacements. The lift is computed using the strip theory (that is, with no assumed aerodynamic interaction between elements) and assuming an instantaneous lift buildup after a change in the angle of attack. Using the strip-theory in aerodynamic calculations tremendously simplifies the aerodynamic calculations and is well justified in large aspect ratio wings such as sailplane wings.

Likewise, the first two terms in the right-hand side of

FIGURE 9:
Displacements of elements of the elastic airplane
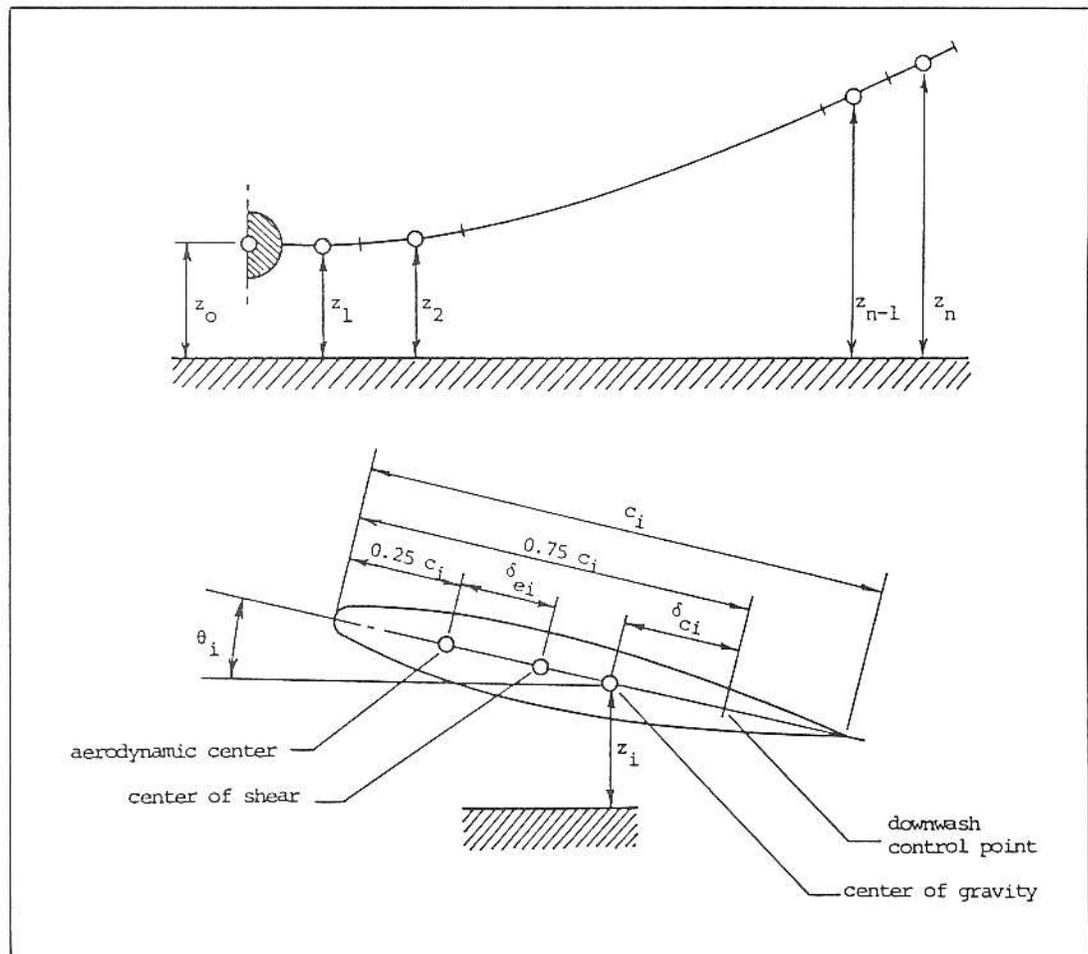
Eq. (27c) represent the elastic restraint moment acting on element i. The fourth term represents the aerodynamic pitching moment due to element motions and displacements.

The third term on the right-hand side of Eq. (27c) is a fictitious damping term. Without this term the elements would experience very lightly damped limit-cycle pitching oscillations every time the sign of the external moment is changed. In a real wing these oscillations would be rapidly attenuated by material damping; in the present calculations this damping term is merely to simulate the material damping effect. A suitable value for the damping factor d has been found to be 0.0001.

Eqs. (27) have been formulated so that they reduce to the rigid-body equations of motion (Eqs. (14)) as the number of wing elements is zero. The fuselage/tail combination is assumed to have no lift as is seen from Eq. (27b). On the other hand, the overall rigid-body pitching moment equilibrium is satisfied by the body element pitching moment equilibrium represented by Eq. (27d).

The stiffness matrix k_{ij} from given wing stiffness data was calculated using the program GUST3STIF. This program defines the wing elements, calculates the masses and moments of inertia of each element and computes the stiffness matrix for an airplane with a rigidly fixed fuselage. These data points are then stored on a file. The mass and stiffness data were taken from Ref. 3 for the PIK-20 and from Ref. 4 for the ALCOR.

Eqs. (27) through (32) were solved with the program GUST3 using a fourth order Runge-Kutta scheme and the file generated by GUST3STIF as input. The program GUST3 transforms the fixed-body stiffness matrix computed by program GUST3STIF to the corresponding free-body stiffness matrix. GUST3 also modifies total mass and wing mass, if necessary.

Some of the results are shown in Figure 10 for the PIK-20 in the same flight condition and for the same gust configuration as in Figure 3, and for the ALCOR in Figure 11. A run for one gust penetration took about 7.5 hours with a time step 0.0001 (this seemed to be about the maximum at which the computation converges).

A comparison between the rigid-body responses and the elastic airplane responses shows that the altitude gain is much larger for the elastic airplane than for the rigid airplane. The velocity increase, on the other hand, is smaller for the elastic airplane. The energy altitude increase seems to be about 15 to 20 percent larger for the elastic airplane. It can thus be concluded that elasticity has a significant effect on the energy gain of a sailplane in a gust.

Another difference is that for the elastic airplane the pitching angle (not shown in Figures 10 and 11) is very small

FIGURE 10: Results of a sample calculation with GUST3 for PIK-20; m = 350 kg, static stability margin = 20% of $\bar{c}$, w_{gn} = 2 m/s, L_{gn} = 50 m, V = 40 m/s. Aerodynamic center at 25% of chord, elastic axis and c.g. axis at 40% of chord; wing mass = 50 kg; z_e = 1.452 m
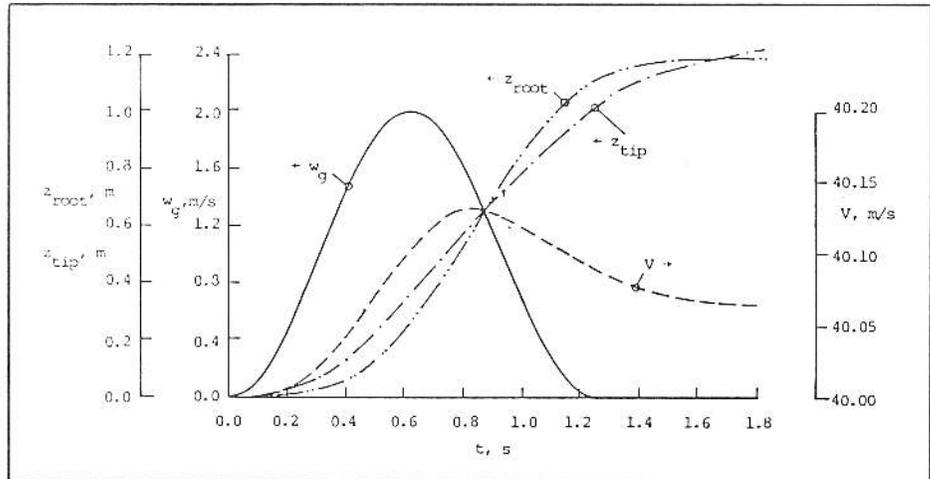
FIGURE 11: Results of a sample calculation with GUST3 for ALCOR; m = 350 kg, static stability margin = 20% of $\bar{c}$, w_{gn} = 2 m/s, L_{gn} = 50 m, V = 40 m/s. Aerodynamic center at 25% of chord, elastic axis and c.g. axis at 40% of chord; wing mass = 83.36 kg; z_e = 1.419 m
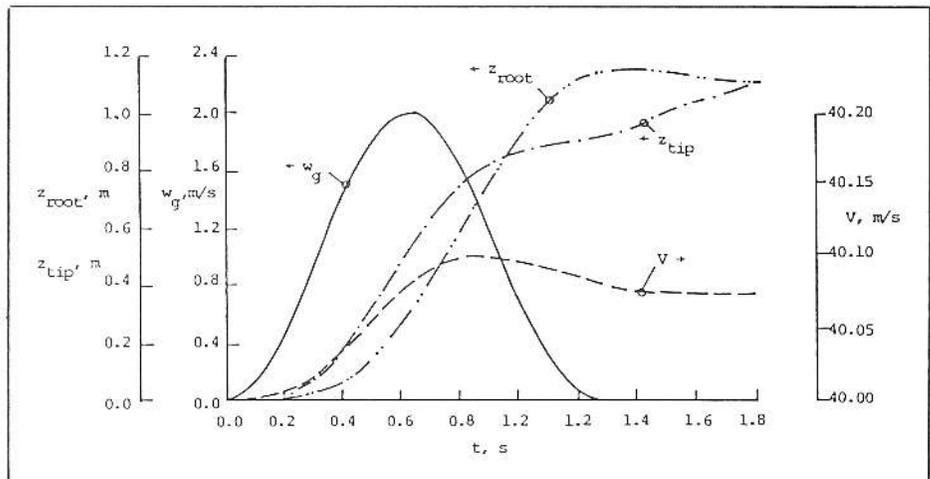
in comparison to the rigid airplane pitching angle; in these particular cases it was only about 0.02 to 0.15 degrees.

Even for the elastic airplane the development of the apparent thrust roughly follows the gust speed. The maximum values were 103.5 N and 78.3 N, respectively, for the PIK-20 and the ALCOR in the cases shown in **Figures 10** and **11**; these could well account for the "gentle push" referred to in the introduction. For higher wing loadings the thrust becomes even higher. E.g. for the PIK-20 with 70 kg water ballast in each wing the maximum thrust was 163.1 N.

A possible explanation for the differences between elastic and rigid-body response could be as follows: The elastic wing bends due to the gust, thus delaying the overall lift build-up; this in turn delays the weathercock effect, diminishing the pitch angle. Here the wing acts like a rapidly responding "energy storage". Later on the energy stored in the bending wing begins to lift the fuselage. However, this occurs relatively late and at this time the gust speed is already diminishing. This in turn causes a negative thrust and consequently a decrease in the flight speed.
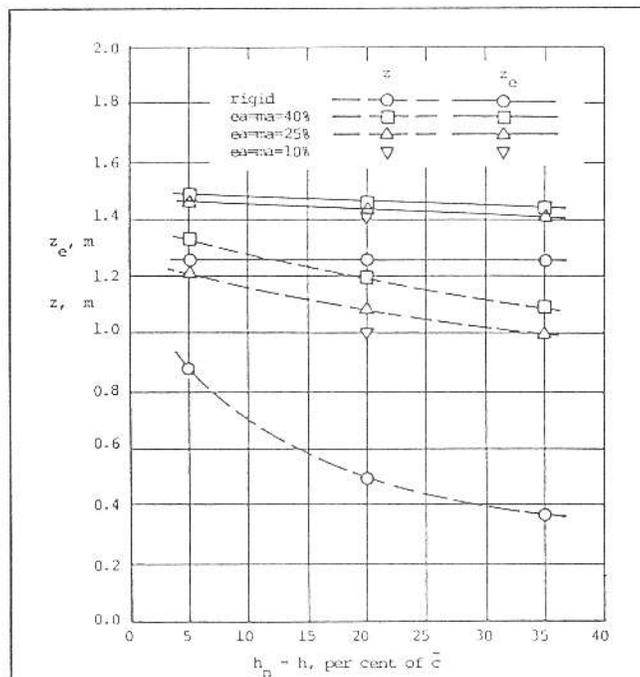
FIGURE 12: Effect of static stability margin on the altitude, velocity and total energy gain of the PIK-20; $w_{gn} = 2$ m/s, $L_{gn} = 50$ m, $V_o = 40$ m/s

Figure 12 shows the effect of the static stability margin on the altitude gain and the energy altitude gain of the elastic PIK-20. The corresponding data for the rigid airplane have been copied from **Figure 4**, for comparison.

It is seen that the altitude gain increases as the center of gravity moves backward toward smaller static stability margins. The same holds true for energy altitude gain, although to a lesser extent. Both altitude and energy altitude gains increase as the elastic axis together with the center of gravity axis are moved backward from the leading edge, although for the energy altitude gain the effect is

quite small. It is interesting to notice that this is opposite to the results obtained in Chapter 4 for the rigidly twisting wing. On the other hand, the present results are in accordance with the well-known beneficial effect of forward elastic axis locations to gust alleviation. Anyway, the wing twisting seems to have a much smaller effect than wing bending to the energy retrieval of a sailplane penetrating a gust.

Calculations also were attempted where the elastic axis was moved forward of the center of gravity axis, but in these cases the calculations did not converge. It is not known whether this is just a property of the computation
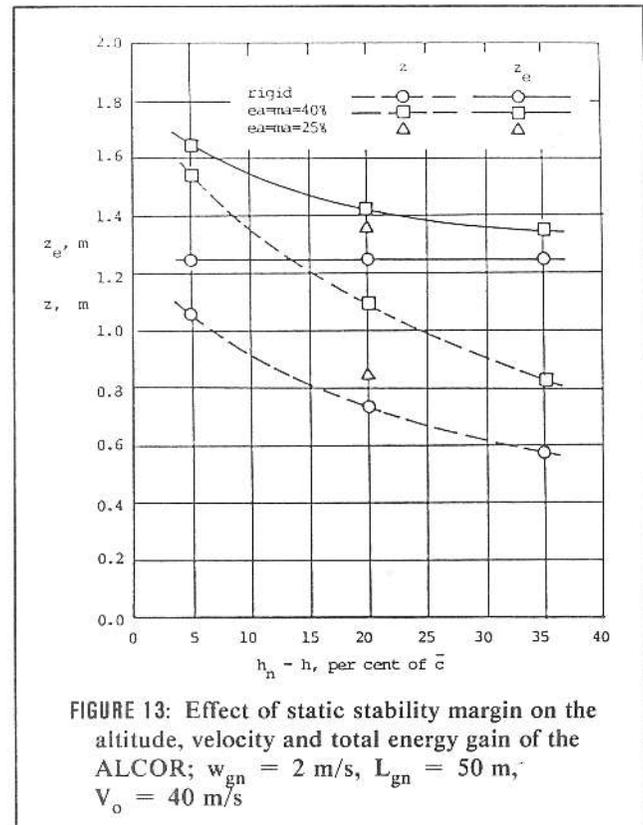
FIGURE 13: Effect of static stability margin on the altitude, velocity and total energy gain of the ALCOR; $w_{gn} = 2$ m/s, $L_{gn} = 50$ m, $V_o = 40$ m/s

algorithm or an indication of true aeroelastic instability. Anyway, it seems that moving the elastic axis forward by means of aeroelastic tailoring without a corresponding modification of the profile center of gravity should be made very cautiously.

A picture corresponding to **Figure 12** for the ALCOR is shown in **Figure 13**. The same general conclusions can be drawn from this picture as from **Figure 12**. The effect of the static stability margin upon altitude gain is much stronger in this case than for the PIK-20; this is probably due to the larger span and a consequently greater wing bending effect at small stability margins.

In addition to a listing of the motions, the program GUST3 also produces a motion data file. This can be used to produce an animation of the motions of the airplane, using the program GUST3PLOT which plots the front view of the airplane and some other data on the screen or on paper with a plotter. A typical output of program GUST3PLOT is seen in **Figure 14**.

PIK-20 EA=MA=40%

VERTICAL SPEEDS

VARIO m/s

GUST m/s

LOCATION

Time = .600 s   V = 40.098 m/s   Zcg = .242 m

Wg = 350 kg   V0 = 40.0 m/s   h0 = 0.0 m

wgust = 2.00 m/s Lgust = 50.00 m   Magnif. = 3.5
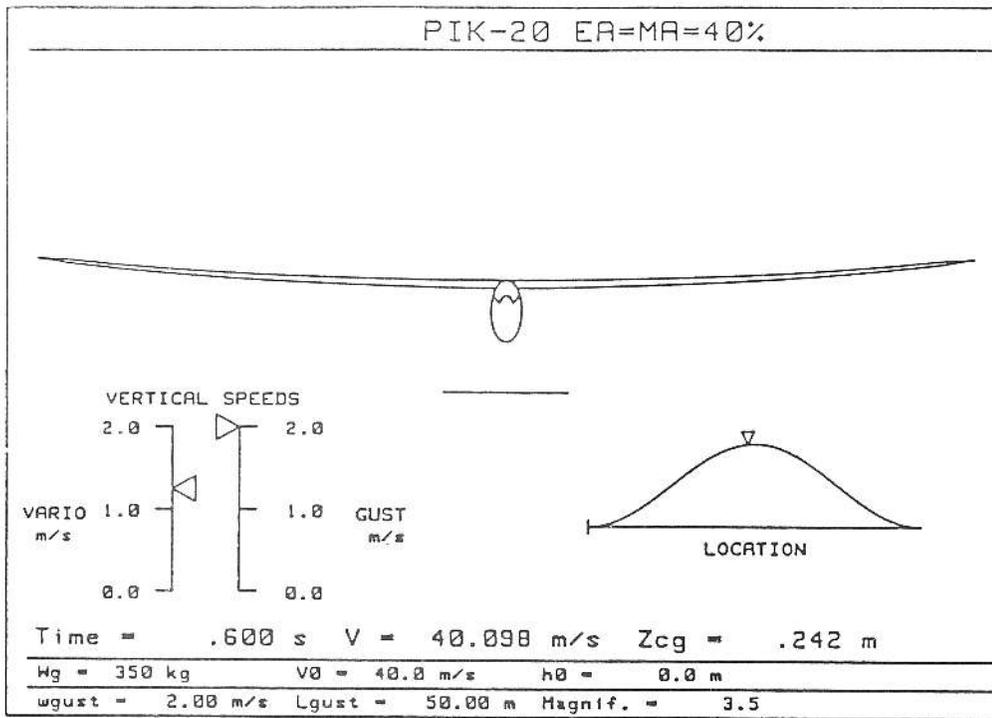
FIGURE 14:

A typical output of program GUST3PLOT

CONCLUSIONS

On the basis of the results obtained, the following conclusions can be made:

—Aeroelasticity has an appreciable effect on the altitude and energy altitude gains of a sailplane penetrating a gust. E.g., for the PIK-20 the energy altitude gain was about 15 to 20 percent higher for the flexible airplane than for the rigid airplane, depending on the center of gravity location. The geometric altitude increase due to aeroelasticity seems to be even higher.

—Most of the altitude and energy altitude gain increase caused by aeroelasticity seems to be due to wing bending coupled with rigid-body pitching: wing flexibility diminishes the weathercock effect, thus allowing a greater lift increase.

—Within certain limits the altitude gain increases as the wing c.g. axis and elastic axis are moved backward with respect to the aerodynamic axis. A similar, although much weaker effect is seen in the energy altitude gain. This suggests that the altitude changes of a sailplane in gusts may be controlled to some extent by aeroelastic tailoring of the wing structure made of composite materials. However, this should be approached very cautiously if the elastic axis is moved forward of the center of gravity axis.

—Both for the rigid airplane and the flexible airplane, the altitude gain increases as the c.g. moves backward toward smaller static stability margins. The same holds true for the energy altitude gain of the flexible airplane, although in this case the effect is less pronounced.

The numeric results obtained in the present treatment should be taken "cum grano salis" because, in order to keep the computational effort at a reasonable level, a number of simplifications were necessary in the mathematical model used. However, the author feels that the general conclusions given above are, in principle, correct.

ACKNOWLEDGMENT

REFERENCES

[1] Lamson, R., Personal communication to the author, Chateauroux, 1978

[2] Etkin, B., "Dynamics of Flight," John Wiley & Sons, Inc., New York, 1959

[3] Korhonen, H., "Lentokoneen aeroelastiset vrhtelyt ja niiden estminen" (Aeroelastic vibrations of an airplane and their prevention, in Finnish), M. Sc. Thesis, Helsinki University of Technology, Department of Mechanical Engineering, Otaniemi, Finland, 1972

[4] Doherty, C.S., "Initial Flutter Studies of the Sailplane 'ALCOR' "